

Supporting Information

Sirtuin Inhibitor Sirtinol is an Intracellular Iron Chelator

Ritika Gautam, Eman A. Akam, Andrei V. Astashkin, Jonathan J. Loughrey and Elisa Tomat*

*Department of Chemistry and Biochemistry
University of Arizona
1306 E. University Blvd., Tucson AZ 85721, USA*

Contents

Experimental Section

- Materials and instrumentation
- Synthesis of complex $[\text{Fe}^{\text{III}}(\text{sirtinol-H})(\text{NO}_3)_2]$
- X-ray diffraction analysis
- Cell culture and preparation of whole-cell EPR samples

Figures S1–S3: UV-visible absorption data

Figure S4: EPR spectroscopy data

Figures S5–S6: X-ray diffraction data

References

Materials and instrumentation. Sirtinol was prepared as previously reported.¹ Tetrahydrofuran (THF) and pentane were dried by passage through a Vacuum Atmospheres solvent purifier. Methanol was freshly distilled and subjected to four freeze-pump-thaw cycles for use in air-free titration experiments. All other reagents were obtained commercially and used as received.

UV-visible absorption spectra were obtained on an Agilent 8453 spectrophotometer equipped with a VWR 1180S temperature controller set at 25.0 °C. For Fe(II) titration experiments, a stock solution of FeCl₂ (25.8 mM) was prepared in dry methanol. Additions (0–3 equiv. Fe(II)) to a sirtinol solution in dry methanol or in a 1:1 mixture of MeOH and buffered water (50 mM PIPES, pH 7.4) were carried out with a glass syringe. After each addition, the solution was allowed to equilibrate.

Solution magnetic moments were measured by the Evans method² using reported diamagnetic corrections.³ Solutions of the ferric complex (5.0 mg/mL in CD₃CN) were transferred into a 5-mm NMR tube and a Wilmad® coaxial insert filled with the deuterated solvent was placed inside as an internal reference. Solution magnetic susceptibilities were calculated based on the difference in chemical shift for the ¹H NMR resonance of the residual solvent protons in neat CD₃CN and in the solution containing the paramagnetic species. ¹H NMR data were recorded at the University of Arizona NMR Facility on a Bruker DRX–500 instrument.

Low- and high-resolution mass spectra were acquired at the University of Arizona Mass Spectrometry Facility. Elemental analysis was performed by Numega Resonance Labs, San Diego, CA. The continuous-wave (CW) EPR experiments were carried out at the University of Arizona EPR Facility on a X-band EPR spectrometer Elecsys E500 (Bruker) equipped with an ESR900 flow cryostat (Oxford instruments).

Synthesis of ferric complex $Fe(C_{26}H_{21}N_2O_2)(NO_3)_2$. Sirtinol (100 mg, 0.25 mmol) was dissolved in THF (20 mL) and solid Fe(NO₃)₃•9H₂O (101 mg, 0.25 mmol) was added. A rapid color change from bright yellow to green was observed and the mixture was allowed to stir for 30 min at room temperature. The solvent was then evaporated under reduced pressure, and recrystallization from THF/pentane gave the ferric complex as a dark green crystalline solid (107 mg, 62%). X-ray quality crystals were obtained by slow diffusion of pentane in a solution of the complex in THF at room temperature. MS-ESI [Fe(C₂₆H₂₁N₂O₂)]⁺ *m/z* 449.09475 (calculated: 449.09470); UV/Vis (CH₃OH): λ_{max} (ε) 329 (15,300), 382 (10,300), 496 (2,100), 581 (1,400); Fe(C₂₆H₂₁N₂O₂)(NO₃)₂•0.5C₄H₈O•0.5C₅H₁₂•3H₂O: C, 52.37 (52.52); H, 5.02 (5.06); N, 7.93 (8.03%); μ_{eff} (Evans method): 6.0 ± 0.1 μ_B.

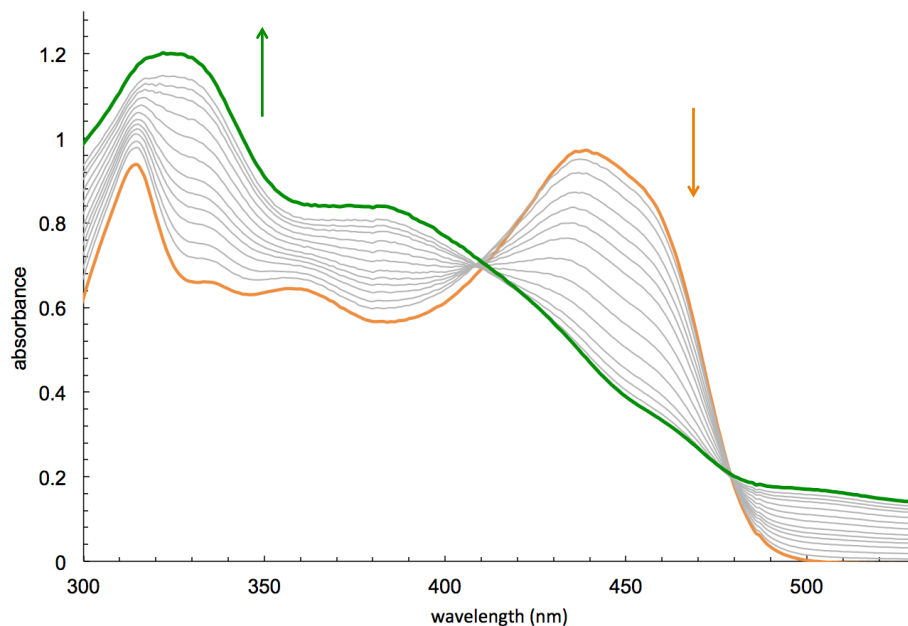


Figure S1. Optical spectral changes occurring after addition of 1 equiv. Fe(II) to a solution of sirtinol (76 μM , orange trace) over a period of 20 min in a 1:1 mixture of MeOH and buffered water (50 mM PIPES, pH 7.4) under an aerobic atmosphere. Additions of 2 or 3 Fe(II) equiv. elicited analogous changes indicating conversion to the same species.

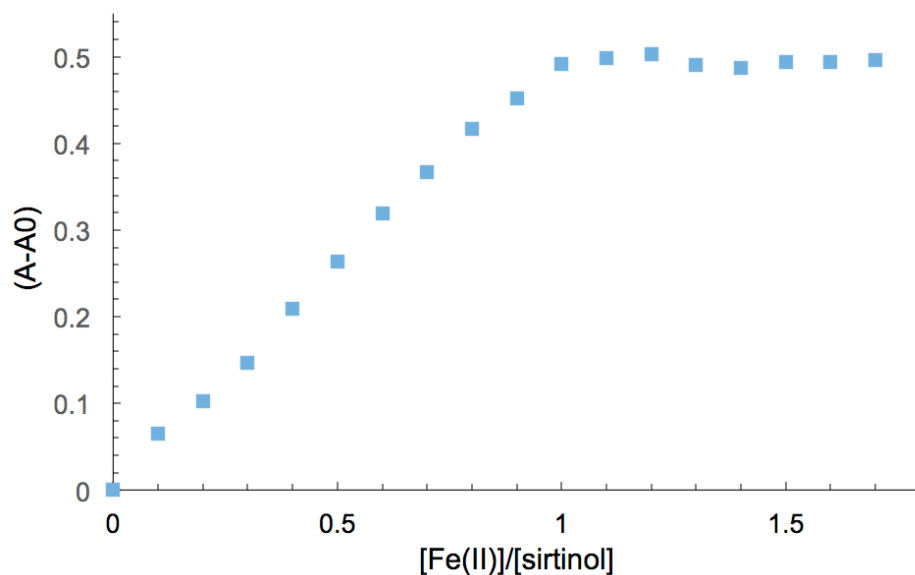


Figure S2. Binding isotherm based on absorbance values at 405 nm for the titration of sirtinol (86 μM) with Fe(II) in MeOH under an argon atmosphere confirming a 1:1 coordination stoichiometry.

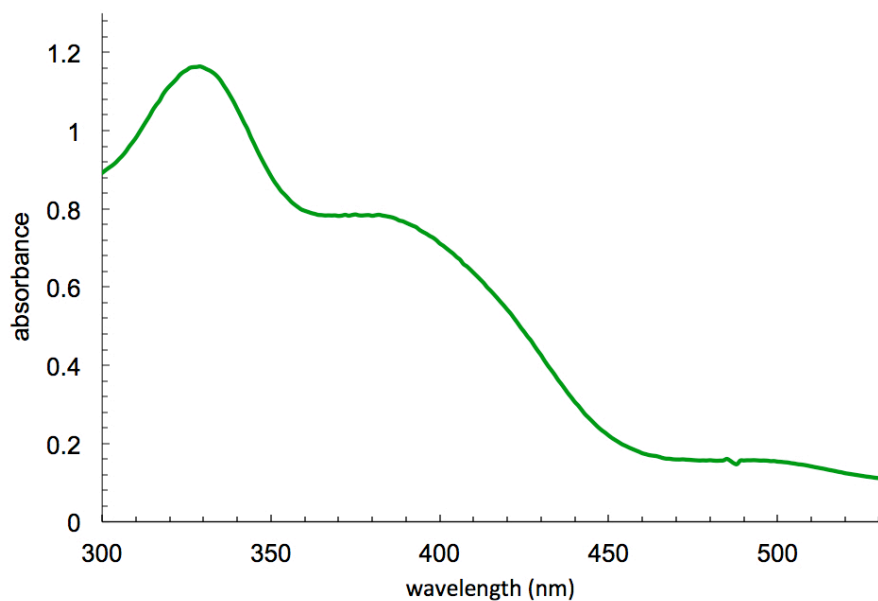


Figure S3. UV/visible absorption spectrum of $[\text{Fe}^{\text{III}}(\text{sirtinol-}H)(\text{NO}_3)_2]$ (in CH_3OH) isolated by crystallization from the reaction of the free ligand with ferric nitrate.

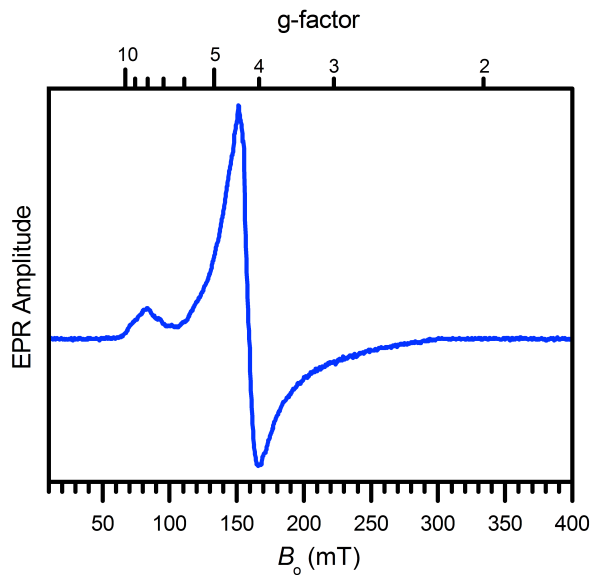


Figure S4. Frozen glass CW-EPR spectrum of $[\text{Fe}^{\text{III}}(\text{sirtinol-}H)(\text{NO}_3)_2]$ in DMSO. This spectrum is characteristic of the high spin ($S = 5/2$) ferric center in rhombic crystal field and shows a major feature at $g = 4.3$ and a minor feature at $g \approx 9$ corresponding to the intermediate and lowest Kramers doublets, respectively. Experimental conditions: microwave frequency, 9.337 GHz; microwave power, 2 mW; magnetic field modulation amplitude, 0.5 mT; temperature, 14 K.

X-ray diffraction analysis. Data were collected at the University of Arizona X-ray Diffraction Facility. Crystals were mounted onto a *MiTeGen* micromount under a protective film of Paratone®, and diffraction data were measured using a Bruker Kappa APEX II DUO diffractometer with graphite-monochromated Mo-K α radiation ($\lambda = 0.71073 \text{ \AA}$) generated by a sealed tube and an APEX II CCD area detector. The diffractometer was fitted with an Oxford Cryostream low-temperature device and the datasets were collected using the *APEX2* software package.⁴ Data were corrected for absorption effects using a multi-scan method in *SADBS*.⁵ Experimental details of the structure determination are given in Table S1. The structure was solved using *Superflip*⁶ and developed by full least-squares refinement based upon F^2 (*ShelXL*).⁷ Crystallographic figures were prepared using *XSEED*,⁸ which incorporates *POVRAY*.⁹

The structure was collected, solved and refined in the chiral monoclinic space group $P2_1$. The asymmetric unit contains two crystallographically independent, fully occupied complex molecules, each containing a seven-coordinate iron(III) center, and three fully occupied tetrahydrofuran molecules with no other significant peaks in the Fourier map. All non-hydrogen atoms were located in the Fourier map and refined anisotropically, while all hydrogen atoms were placed in calculated positions and refined using a riding model.

The THF molecules exhibited large differences between internal bond lengths therefore they were refined with the restraints $C-C = C-O = 1.45(2) \text{ \AA}$. Although these solvent molecules remained substantially disordered, there was no significant departure from expected bond lengths within the aromatic portions of the independent, coordinated sirtinol molecules. The absolute configuration of the compound was confirmed by the value of the Flack parameter, found to be 0.006(12). The highest residual Fourier peak was $+0.54 e.\text{\AA}^{-3}$ located approx. 1.3 \AA from O65 on one of the THF molecules and likely due to disorder in the molecule which could not be modeled. The deepest Fourier hole was $-0.38 e.\text{\AA}^{-3}$ approx. 0.93 \AA from O65.

Two hydrogen bonding interactions between THF oxygen atoms O60 and O70 and amide hydrogen atoms H6 and H2A, respectively, of the coordinated sirtinol moieties (Fig. S6) hold the THF molecules in a small solvent pocket between adjacent complexes.

The iron centers present a slightly distorted pentagonal bipyramidal geometry, with equatorial angles adding up to 359.98° and 359.97° and axial angles to the amidic carbonyl and phenoxide oxygen donors adding to $174.554(4)^\circ$ and $174.5752(2)^\circ$ for Fe1 and Fe2, respectively. The iron-centered bond lengths are in the range expected for a d^5 high-spin iron(III) complex ($S = 5/2$) with similar ligands.¹⁰

Crystal data for $C_{64}H_{66}Fe_2N_8O_{19}$, $M_r = 1362.95$, $0.1 \times 0.05 \times 0.05$ mm, monoclinic, space group $P2_1$, $V = 3166.2(2) \text{ \AA}^3$, $Z = 2$, $\rho_{\text{calc}} = 1.430 \text{ g/cm}^3$, $F_{000} = 1420$, Mo-K α radiation, $\lambda = 0.71073 \text{ \AA}$, $T = 150(2) \text{ K}$, $2\theta_{\text{max}} = 50.1^\circ$, 23819 reflections collected, 10735 unique ($R_{\text{int}} = 0.0353$). Final $Goof = 1.017$, $R_I = 0.0404$, $wR_2 = 0.0924$, R indices based on 8266 reflections with $I > 2\sigma[I]$ (refinement on F^2), Flack parameter = 0.006(12). Lp and absorption corrections applied, $\mu = 0.539 \text{ mm}^{-1}$.

Table S1. Crystal data and structure refinement.

	[Fe(C₂₆H₂₁N₂O₂)(NO₃)₂]₂•3[C₄H₈O]
Molecular formula	$C_{64}H_{66}Fe_2N_8O_{19}$
Formula weight [g.mol ⁻¹]	1362.95
Temperature [K]	150(2)
Crystal class	monoclinic
Space group	$P2_1$
a [Å]	8.4996(3)
b [Å]	14.4218(7)
c [Å]	26.0595(11)
α [°]	90.00
β [°]	97.616(2)
γ [°]	90.00
Volume [Å ³]	3166.2(2)
Z	2
ρ_{calc} [g/cm ³]	1.430
μ [mm ⁻¹]	0.539
F(000)	1420
Crystal size [mm]	$0.1 \times 0.05 \times 0.05$
Measured reflections	23819
Independent reflections	10735
Independent reflections, $I > 2\sigma[I]$	8266
R_{int}	0.0353
Goodness-of-fit on F^2	1.017
R_1 , $I > 2\sigma[I]^a$	0.0404
wR_2 , all data ^b	0.0924
peak/hole [$e \text{ \AA}^{-3}$]	0.54 / -0.38 $e \cdot \text{\AA}^{-3}$
Flack parameter	0.006(12)

$$^a R = \sum[|F_o| - |F_c|] / \sum |F_o|$$

$$^b wR = [\sum w(F_o^2 - F_c^2) / \sum wF_o^4]^{1/2}$$

Table S2. Selected bond lengths

Fe(1)-O(1)	1.889(2) Å	Fe(1)-O(2)	2.011(2) Å
Fe(1)-O(3)	2.243(3) Å	Fe(1)-O(4)	2.133(3) Å
Fe(1)-O(6)	2.222(3) Å	Fe(1)-O(7)	2.103(3) Å
Fe(1)-N(1)	2.072(3) Å	Fe(2)-O(9)	1.875(2) Å
Fe(2)-O(10)	1.974(2) Å	Fe(2)-O(11)	2.227(3) Å
Fe(2)-O(12)	2.150(3) Å	Fe(2)-O(14)	2.242(3) Å
Fe(2)-O(15)	2.092(3) Å	Fe(2)-N(5)	2.107(3) Å
O(1)-C(1)	1.312(4) Å	O(2)-C(18)	1.268(4) Å
N(1)-C(11)	1.309(5) Å	N(1)-C(12)	1.426(4) Å
N(2)-C(18)	1.310(4) Å	N(2)-C(19)	1.464(4) Å
N(5)-C(37)	1.309(5) Å	N(5)-C(38)	1.428(4) Å
N(6)-C(44)	1.310(4) Å	N(6)-C(45)	1.473(5) Å

Table S3. Selected bond angles

N1-Fe1-O6	81.4654(11) °
O6-Fe1-O7	59.416(2) °
O7-Fe1-O4	78.172(3) °
O4-Fe1-O3	58.8309(17) °
O3-Fe1-N1	82.0923(6) °
O1-Fe1-O1	87.5505(19) °
N1-Fe1-O2	87.003(2) °
Sum of angles around pentagonal plane	359.98 °
N5-Fe2-O11	81.3521(7) °
O11-Fe2-O12	58.8365(18) °
O12-Fe2-O15	77.723(3) °
O15-Fe2-O14	59.021(2) °
O14-Fe2-N5	83.0344(10) °
O9-Fe2-N5	87.5279(19) °
N5-Fe2-O10	88.0313(19) °
Sum of angles around pentagonal plane	359.97 °

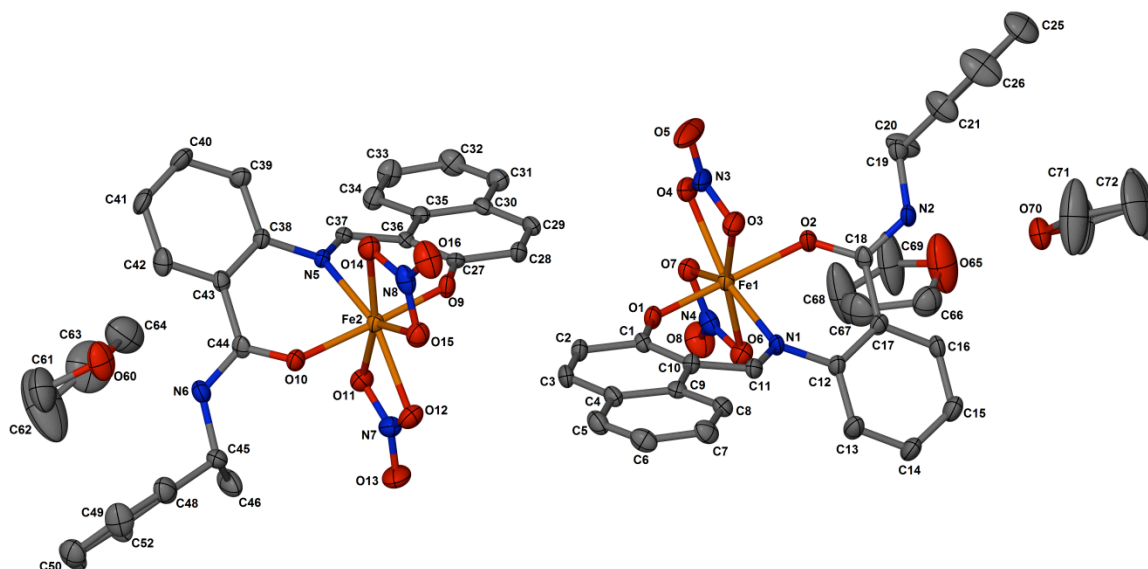


Figure S5. Asymmetric unit of $[\text{Fe}^{\text{III}}(\text{sirtinol-H})(\text{NO}_3)_2] \cdot 3(\text{THF})$ showing the full labelling scheme. All atoms are displayed as thermal ellipsoids at 50% probability. All hydrogen atoms are omitted for clarity. C26 is hidden behind C21, C24 is hidden behind C26, C73 is hidden behind C72 and C74 is hidden behind C71.

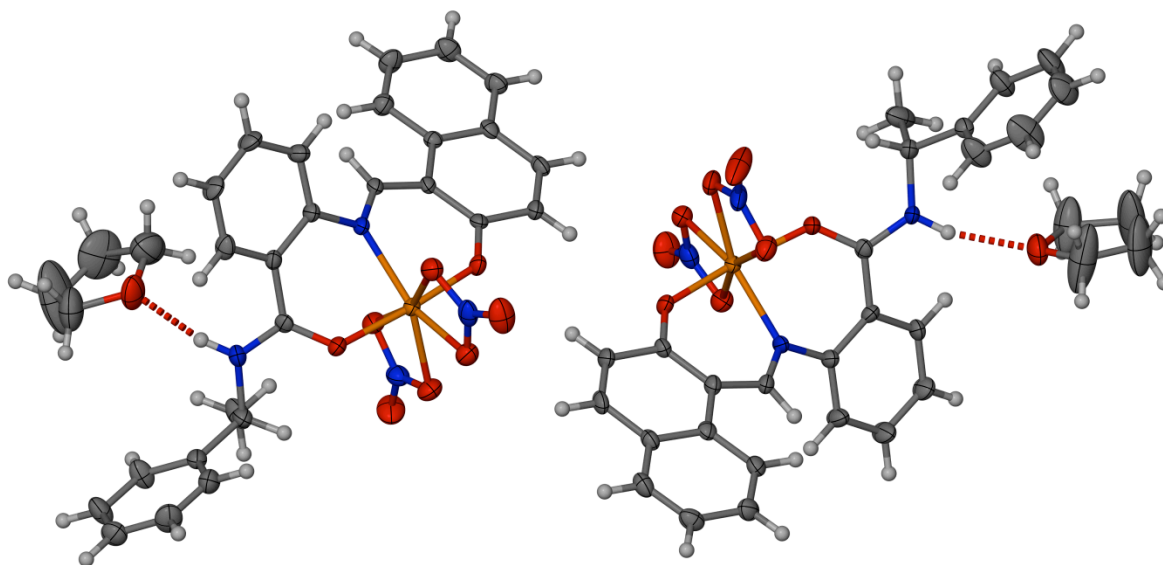


Figure S6. View of the asymmetric unit (minus one tetrahydrofuran molecule) highlighting the hydrogen-bonding interactions between the complexes and two tetrahydrofuran molecules. All non-hydrogen atoms are shown as their thermal displacement ellipsoids.

Cell culture and preparation of whole-cell EPR samples. Human Jurkat T cells (ATCC® T1B-152™, acute T cell leukemia) were cultured at 37 °C under a 5% CO₂ humidified atmosphere in RPMI 1640 medium supplemented with 10% FBS, 5 mg/ml penicillin, and 1 mg/ml streptomycin and maintained at a density less than 2.0 × 10⁶ cells/mL.

For EPR experiments, Jurkat cells were cultured to a density of 1.8 × 10⁶ cells/mL, treated with the test compounds and incubated for 3 h. The suspension (90 mL) was then centrifuged (1000 rpm, 10 min) to remove treatment medium, and the cells were washed by resuspension in PBS followed by pelleting (1000 rpm, 10 min). After removal of the supernatant, the pellet was suspended in a buffered aqueous solution (200 μL, 50 mM HEPES, pH 6.9, 10% glycerol), transferred to an EPR tube and spun down (1000 rpm, 10 min). The pellet was then quickly frozen in cold methanol (−40 °C) and stored in liquid nitrogen. The total time between the first centrifugation and freezing was less than 30 min.

References

1. A. Mai, S. Massa, S. Lavu, R. Pezzi, S. Simeoni, R. Ragno, F. R. Mariotti, F. Chiani, G. Camilloni, D. A. Sinclair, *J. Med. Chem.* **2005**, *48*, 7789-7795.
2. (a) D. F. Evans, *J. Chem. Soc.* **1959**, 2003-2005; (b) E.M. Schubert, *J. Chem. Ed.* **1992**, *69*, 62.
3. G.A. Bain, J.F. Berry, *J. Chem. Ed.* **2008**, *85*, 532-536.
4. (a) Bruker (2007). *APEX2*. Bruker AXS Inc., Madison, Wisconsin, USA; (b) Bruker (2007). *SAINT*. Bruker AXS Inc., Madison, Wisconsin, USA.
5. G. M. Sheldrick, (1996). *SADABS*. University of Göttingen, Germany.
6. L. Palatinus, G. Chapuis, *G. J. Appl. Cryst.* **2007**, *40*, 786–790.
7. (a) G. M. Sheldrick, *SHELXS97* and *SHELXL97* Programs for Crystal Structure Solution and Refinement, University of Göttingen, Germany, 1997; (b) G. M. Sheldrick, *Acta Crystallogr., Sect. A*, **2008**, *64*, 112-122.
8. L. J. Barbour, *J. Supramol. Chem.* **2001**, *1*, 189-191.
9. Persistence of Vision Pty. Ltd., 2004, Persistence of Vision Raytracer (Version 3.6) Williamstown, Victoria, Australia.
10. (a) D. R. Richardson, P. V. Bernhardt, *J. Biol. Inorg. Chem.* **1999**, *4*, 266-273; (b) S. Avramovici-Grisaru, S. Sarel, S. Cohen, R.E. Bauminger, *Isr. J. Chem.* **1985**, *25*, 288-292; (c) T. Weyhermüller, R. Wagner, B. Biswas, P. Chaudhuri, *Inorg. Chim. Acta* **2011**, *374*, 140-146.